Annu. Rev. Biochem. 1989. 58:223–56

TWO-DIMENSIONAL NMR AND PROTEIN STRUCTURE[1,2]

Ad Bax

Laboratory of Chemical Physics, National Institute of Diabetes and Digestive and Kidney Diseases, National Institutes of Health, Bethesda, Maryland 20892

CONTENTS

PERSPECTIVES AND SUMMARY 224
NMR OF PROTEINS 225
Resonance Assignment of Proteins 227
Through-Bond Correlation 227
Through-Space Correlation 230
Measurement of J Couplings 235
Stereospecific Assignment of Methylene and Methyl Resonances 237
Accuracy of NMR Distance Determination 239
Determination of Tertiary Structure 240
Quality of NMR Structures 243
PROSPECTS FOR THE STRUCTURE DETERMINATION OF LARGER PROTEINS 244
Double Labeling with ^{13}C and ^{15}N 246
^{2}H Labeling 246
Isotope-Edited Experiments 248
^{13}C and ^{15}N Experiments 248
Three-Dimensional NMR 250
DISCUSSION 250

[1]The US government has the right to retain a nonexclusive, royalty-free license in and to any copyright covering this paper.

[2]Abbreviations used: NMR, nuclear magnetic resonance; 1D, one-dimensional; 2D, two-dimensional; 3D, three-dimensional; BPTI, basic pancreatic trypsin inhibitor; TSP, trimethylsilylpropionate; ppm, parts per million; NOE, nuclear Overhauser enhancement; NOESY, 2D NOE spectroscopy; HOHAHA, homonuclear Hartmann-Hahn spectroscopy; TOCSY, total correlation spectroscopy; COSY, homonuclear J-correlated spectroscopy; E-COSY, exclusive COSY; PE-COSY, primitive E-COSY; RMSD, root-mean-square deviation; MD, molecular dynamics; RMD, restrained molecular dynamics; DG, distance geometry; CPI, carboxypeptidase inhibitor; BSPI-2, barley serine proteinase inhibitor 2; EGF, epidermal growth factor

PERSPECTIVES AND SUMMARY

Dramatic improvements in NMR methodology and instrumentation over the past 10 years have made it possible to determine the three-dimensional structures of small proteins in solution. The most important methodological development was the introduction of two-dimensional (2D) NMR, first proposed in 1971 (1) and finding widespread use about a decade later, after instrumental and computer requirements became available for this new class of experiments. 2D NMR spreads the severely overlapping one-dimensional NMR spectrum of a protein into two orthogonal frequency dimensions, giving the NMR spectrum an appearance that is somewhat similar to two-dimensional gel-electrophoresis maps. The resulting improvement in resolution has been a key factor in the detailed NMR structural studies conducted at present. Major instrumental developments concern the increase in magnetic field strength, leading to improved resolution of the ^{1}H NMR spectrum. This increase in field strength, combined with improved radiofrequency technology, has also led to a large increase in NMR sensitivity, needed for the study of proteins at millimolar concentrations.

Much of the early NMR structural work concentrated on BPTI, a small globular protein of 58 amino acids for which a high-resolution X-ray crystallographic structure was available. These initial studies set the ground rules for protein structure determination by NMR (2–9). A significant number of NMR structures have recently become available, although the resolution of many is poor in comparison with high-resolution crystal structures. Often, only the backbone conformation was given, and NMR spectra were too complex to derive complete side-chain definition. More recently, however, improvements in methodology, instrumentation, and data analysis have made it possible to determine NMR structures for small globular proteins with a precision that may be roughly comparable to an X-ray crystal structure determined at 2–2.5 Å resolution.

NMR enables for the first time the study of proteins in their "natural state," at physiological ionic strength and concentration, undistorted by crystal packing forces. This may provide new insights into the rules governing protein structure, function, and dynamics as well as in the protein folding problem. Because the number of new NMR protein structures appears to be growing at an exponential rate, this article is limited to surveying the strategy used for NMR structure determination, its power and limitations, and the prospects for structural studies of proteins significantly larger than 100 amino acids. Recently, a monograph (10) and several reviews have appeared dealing with the structure determination of proteins by NMR (11–13). In addition, a much larger body of review literature is available describing many of the modern NMR techniques used in this structure determination process (14–22).

NMR OF PROTEINS

In order to record NMR spectra of sufficient quality for detailed NMR structural studies, sample concentrations of at least 1 millimolar in 0.5 ml solution are required. The protein should be stable for at least 24 hours at or near room temperature, and the protein should be in the monomeric or at most dimeric form. This last restriction is imposed by the required tumbling rate of the protein that should be described by a correlation time, τ_c, shorter than about 10 ns (τ_c is approximately the time needed to change the protein orientation by one radian). For proteins, the higher the temperature and the lower the apparent molecular weight, the narrower the width of individual proton resonances. Narrow individual resonances are essential for the accurate measurement of the NMR parameters needed for detailed structural studies.

Figure 1 shows three one-dimensional (1D) NMR spectra of polypeptides of different molecular weights, recorded at a magnetic field strength that corresponds to a ^1H resonance frequency of 600 MHz, the highest field strength commercially available to date. For the small magainin-2 peptide (23 amino acids), many of the resonances, each originating from a particular proton in the peptide, are well resolved. For the larger BPTI (6.5 kd) and staphylococcal nuclease (18 kd), much smaller fractions of the protons yield nonoverlapping resonances. The resonance position in the spectrum reflects the shielding of the nucleus by the surrounding electrons, i.e. it reflects the electron density at the position of the nucleus (23a, 23b). Amide and aromatic protons are, on average, most deshielded and their resonance frequencies are about 6–10 ppm higher relative to a commonly used reference signal from the methyl protons in trimethylsilylpropionate (TSP). Note that according to NMR convention, frequency increases toward the left of the spectrum. CαH protons typically resonate between 3 and 5 ppm and methyl groups between 0 and 2 ppm. Differences in chemical shifts between two amide protons, for example, are caused by structural differences in their vicinity. However, to date, no clear correlation between local structure and chemical shift is available (24a, 24b).

Expansions of the 1D spectra in Figure 1 show small splittings for each of the resonances. These so-called J splittings are caused by a scalar interaction (J coupling) with neighboring protons, two or three chemical bonds removed. The absolute size of the couplings reflects the torsion angle between the C or N nuclei to which the hydrogens are attached.

A second, even more important source of structural information stems from the fact that the protons continuously exchange their nuclear magnetization with one another, at rates that depend on the sixth power of their interspatial distance, r^{-6}. By measuring these magnetization exchange rates, a set of

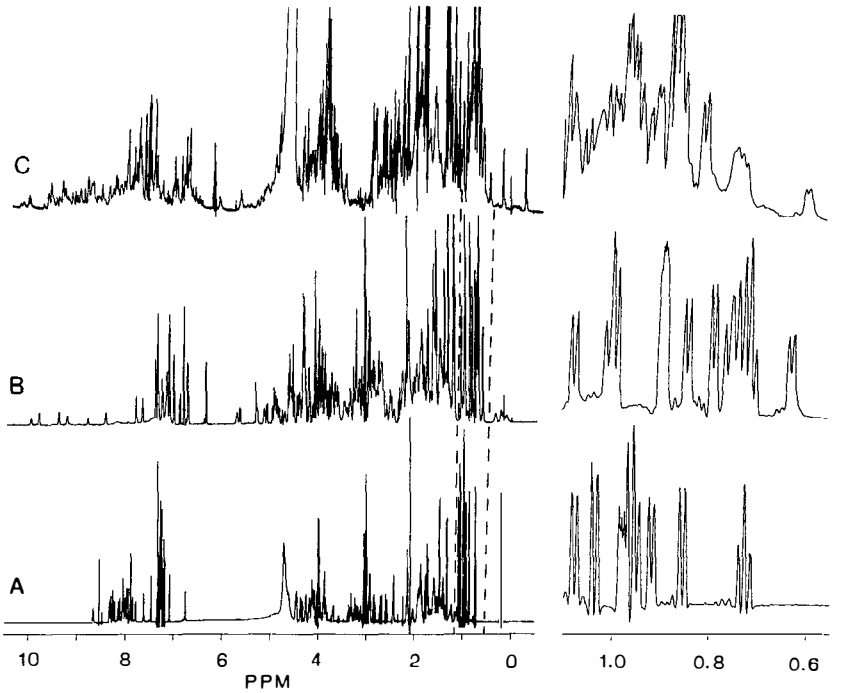

Figure 1 ^{1}H NMR spectra of (*A*) magainin 2 (23 amino acids) in 75% H_2O, 25% trifluoroethanol-d_3, (*B*) basic pancreatic trypsin inhibitor (58 amino acids) in ^2H_2O, and (*C*) staphylococcal nuclease (156 amino acids) in 90% H_2O/10% ^2H_2O. All spectra were recorded at 27°C at 600 MHz and identical digital filtering was used for all three spectra to sharpen the individual resonances. Note that because of hydrogen exchange most but not all amide protons are replaced by deuterons in the BPTI spectrum. In the expansions of the regions between the broken lines, shown on the right, J splittings of the resonances are observed.

interproton distances is obtained. This magnetization exchange is often referred to as the nuclear Overhauser effect (NOE) (25), and the most convenient method for measuring it is called the NOESY (NOE *s*pectroscop*y*) experiment (26, 27).

Other structural information can be derived from amide hydrogen exchange rates, which depend strongly on solvent accessibility and hydrogen bonding. It is well established that hydrogen-bonded amide protons are less labile than non–hydrogen-bonded ones (3, 28, 29). By dissolving the protein in D_2O solution, one can monitor which resonances disappear most slowly and thereby obtain information about the hydrogen bonding patterns in the protein. For example, the spectrum in Figure 1*b* has been recorded about one year after the protein was dissolved in D_2O, and all non–hydrogen-bonded plus many hydrogen-bonded protons were exchanged with solvent deuterons at the time this spectrum was recorded.

All structural information mentioned above becomes available only once firm individual resonance assignments have been established. The assignment procedure is one of the most difficult and tedious steps in protein structure determination. Below, various methods used for obtaining resonance assignments will be briefly discussed.

Resonance Assignment of Proteins

Wüthrich and coworkers have developed a standard approach for systematic resonance assignments in proteins (2, 6, 7, 30). However, it should be realized that in practice a pure systematic approach often will be insufficient for all but the smallest proteins and slightly modified procedures are often followed (31). Nevertheless, for conceptual reasons it may be useful to consider this standard assignment recipe.

The first step in the resonance assignment uses J-coupling (through-bond) information to classify resonances according to which type of amino acid they correspond. For example, glycine is the only residue where two protons interact with the amide proton, and alanine is the only residue where the CαH interacts directly with methyl protons. In contrast, His, Trp, Tyr, and Phe residues are difficult to distinguish because in each case, the CαH interacts with two Cβ methylene protons that do not show any J coupling to any of the ring protons (more than three bonds removed). Therefore, these residues are also difficult to distinguish from Asp, Asn, Cys, and Ser residues.

The second step in the assignment procedure concerns the identification of the sequence-specific position of each amino acid, relying on through-space connectivity provided by the NOESY experiment. As will be discussed later, for any peptide backbone conformation, NOE interactions between adjacent amino acids are prescnt, making it possible to search for unique dipeptide segments in the protein backbone (provided its sequence is known). Such unique dipeptides then present starting points for further sequential resonance assignments based on the NOESY experiment.

Through-Bond Correlation

A series of two-dimensional NMR experiments have been developed that permit identification of J-coupled protons (1, 32–45). The simplest such experiment is depicted in Figure 2a. In this COSY experiment, two radiofrequency pulses are applied, spaced by a variable time, t_1. Fourier transformation of the time domain data collected after the second pulse, during the time t_2, results in ^{1}H NMR spectra, in which the intensities of the individual resonances are sinusoidal functions of the time t_1. A particular resonance is modulated as a function of t_1 not only by its own chemical shift frequency, but also by the frequencies of protons that have a J coupling to the proton of interest. By repeating the pulse scheme of Figure 2 for a large number of different t_1 durations, it becomes possible to determine all modulation

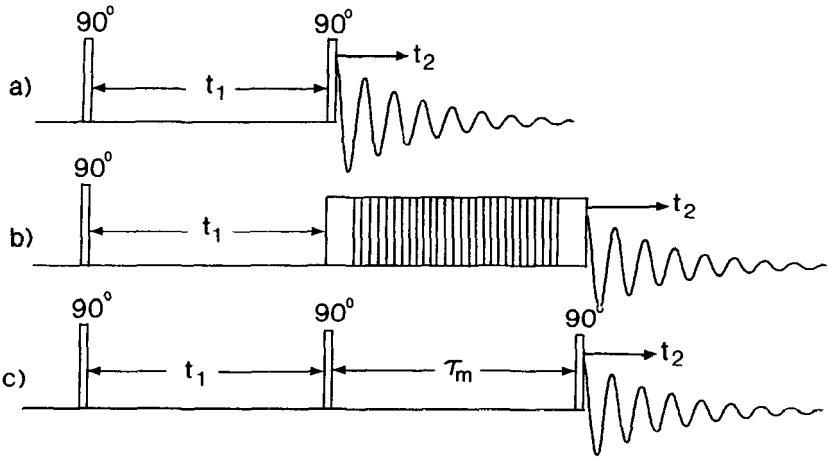

Figure 2 Pulse schemes of three of the most commonly used 2D NMR experiments: (*a*) the COSY experiment, (*b*) the HOHAHA experiment, and (*c*) the NOESY experiment. For each value of t_1, a spectrum is obtained by Fourier transformation of the data acquired during the time t_2. In consecutive experiments, t_1 is systematically incremented from 0 to about 100 ms, in steps of about 200 μs.

frequencies present for a particular resonance, i.e. the resonance frequencies of all J-coupled protons. This is done most easily using a two-dimensional Fourier transformation with respect to the time variables, t_1 and t_2, resulting in a frequency domain spectrum with frequency variables F_1 and F_2.

An example of such a spectrum, obtained for the antimicrobial peptide magainin 2 (46), is shown in Figure 3*a*. Information particularly important for resonance assignment is contained in the boxed region connecting the amide and the CαH protons. An expansion of this so-called fingerprint region (Figure 3*b*) shows a single correlation for each amino acid, with the exception of glycine residues where the NH proton shows a correlation to two Cα protons. Note that although all so-called cross peaks in the spectrum of Figure 3*b* have been labeled, the only residues that can immediately be identified from this part of the spectrum are the glycine residues. For type-specific assignments of the other amino acids, connectivity information between the CαH and side chain protons is needed. Thus, it is seen from Figure 3*a* that a CαH proton at 4.22 ppm correlates with a methyl group at 1.51 ppm, assigning these resonances to an Ala residue. Note that proline is the only amino acid that does not contain an amide hydrogen and this residue does not yield any resonances in the fingerprint region.

The CαH of the second Ala residue (A15) resonates at exactly the same position as CαH of E19, making identification of the NH proton of this second Ala residue ambiguous. However, a number of experimental techniques are available that can provide indirect or relayed connectivity. One

such technique, referred to as homonuclear Hartmann-Hahn (HOHAHA) (38) or total correlation spectroscopy (TOCSY) (37), in principle permits the correlation of all protons within a given coupling network. A small region of such a HOHAHA spectrum, recorded for the protein hirudin (65 amino acids) displaying connectivities between NH protons and CαH and side chain protons, is shown in Figure 4. The spectrum has been recorded for a mixing time of 50 ms, sufficiently long for yielding a substantial number of HN-CβH and NH-CγH connectivities. Because of the absence of J coupling between the $C\beta H_2$ and the ring protons, connectivities between NH protons and ring protons of the Phe and His residues are usually not observed. This HOHAHA experiment, first applied to proteins by Clore, Gronenborn, and coworkers (47, 48), is rapidly gaining popularity.

The pulse scheme used in the HOHAHA experiment is quite complex, as depicted in Figure 2*b*. The second pulse in the COSY pulse scheme of Figure 2*a* now has been replaced by an integral number of repetitions of 49 pulses (38). These pulses are timed in such a way that during their application the effect of chemical shifts is temporarily removed. This then permits magnetization to flow freely from one proton to another, at a rate determined by their J coupling. As pointed out above, the HOHAHA experiment can remove ambiguities arising from coincident chemical shifts. In addition, this experiment offers relatively high sensitivity and resolution compared to the hitherto more commonly used COSY technique. For a detailed discussion of theoretical and experimental aspects of this class of experiments, the reader is referred to the literature (37–40).

A third class of experiments utilizes multiple-quantum transitions; these are transitions in which several nuclei participate simultaneously in a coherent manner (15, 41, 49–54). The multiple-quantum frequency itself can be measured (53, 54), which is always a linear combination of the resonance frequencies of the nuclei participating in such a transition. Alternatively, experiments exist that use special properties of multiple-quantum transitions to select certain types of amino acids that are capable of generating such a multiple-quantum transition (41, 49–52). For example, since glycine has only two coupled protons, assuming that the NH protons have been exchanged for deuterons, no triple-quantum transitions can be generated, and a spectrum free of glycine resonances can be obtained by using a so-called triple-quantum filter (41, 49). At first sight these multiple-quantum filtered spectra have the same appearance as regular COSY spectra. However, a closer inspection shows cross peak patterns that are characteristic for the type of amino acid (51, 52). The most popular of such filtered experiments are the double-quantum and triple-quantum filtered COSY experiments, although higher orders of filtering have also been demonstrated for small model compounds. In general, higher orders of multiple-quantum filtering result in simpler spectra but also in a lower signal-to-noise ratio.

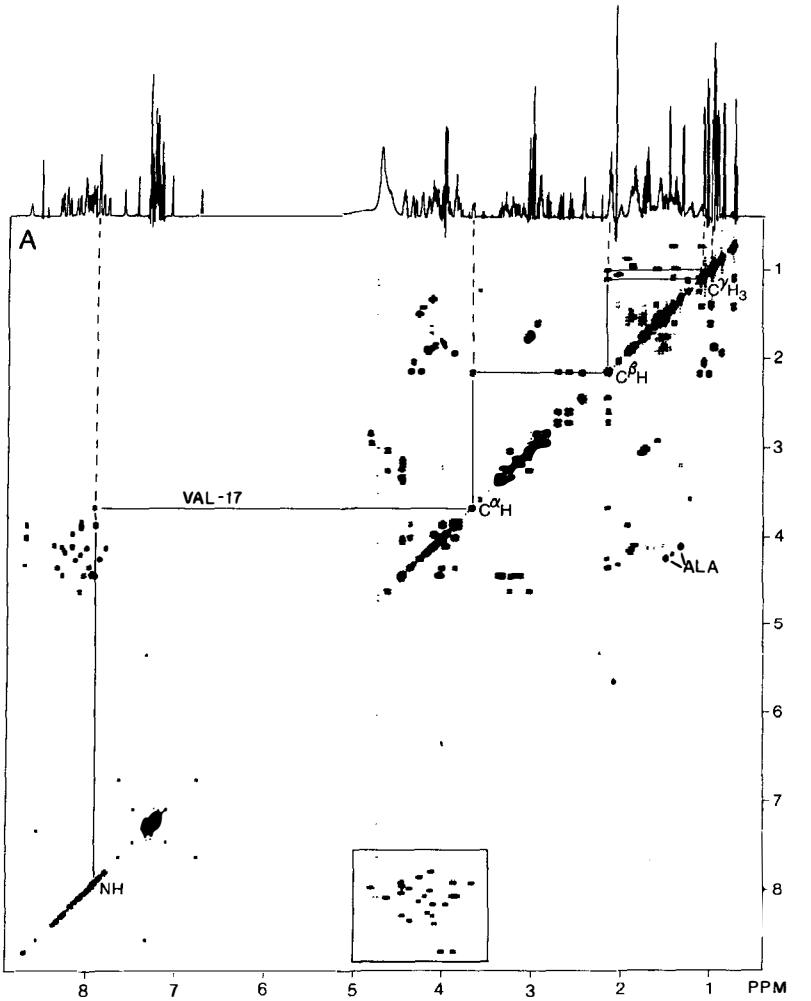

All COSY, multiple-quantum, and HOHAHA correlation techniques are limited to cases where the line width is not much larger than the size of the J coupling. For proteins larger than about 20 kd, this is no longer the case and these valuable sources of information disappear. Even for smaller proteins, it rapidly becomes more difficult to observe NH to side chain connectivities when the temperature is decreased (i.e. the viscosity and τ_c are increased).

Through-Space Correlation

After the J-correlated types of experiments have identified sets of J-coupled NH, CαH, and CβH resonances for the individual amino acids, it becomes

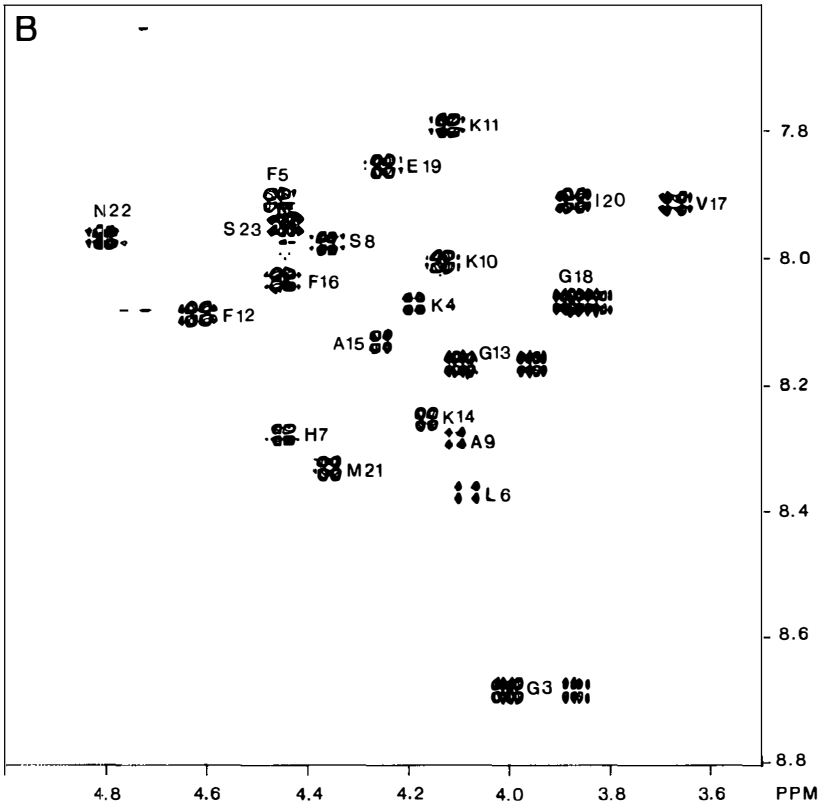

Figure 3 (*A*) 600 MHz COSY spectrum of 12 mg magainin 2 in 0.5 ml 75% H_2O/25% trifluoroethanol-d_3. The drawn lines in (*A*) identify the coupled protons of Val-17. CαH-CH_3 cross peaks of the two alanine residues are marked Ala. The boxed region (commonly known as the "fingerprint region") shows interactions between NH and CαH protons and is enlarged in (*B*). In this enlargement a single cross multiplet, consisting of a number of closely spaced multiplet components, is observed for each nonglycine amino acid with the exception of the two N-terminal residues, for which the NH protons exchange rapidly with the solvent. For glycine residues, two cross peaks are observed corresponding to the two nonequivalent CαH protons. For Gly-18, the chemical shifts of the two CαH protons differ by only 0.04 ppm, and the two multiplets nearly overlap. For both Gly-3 and Gly-13 the CαH chemical shifts differ by about 0.2 ppm, and the label is positioned in between the two cross peaks.

necessary to identify every amino acid not only by type, but also regarding its position in the polypeptide sequence. Most commonly this information is derived from NOESY experiments that yield 2D spectra that show correlations for pairs of protons that are in close proximity of each other. Most of such NOE correlations are short range, i.e. they correspond to protons that are less than five amino acids apart in the peptide sequence. However, a sub-

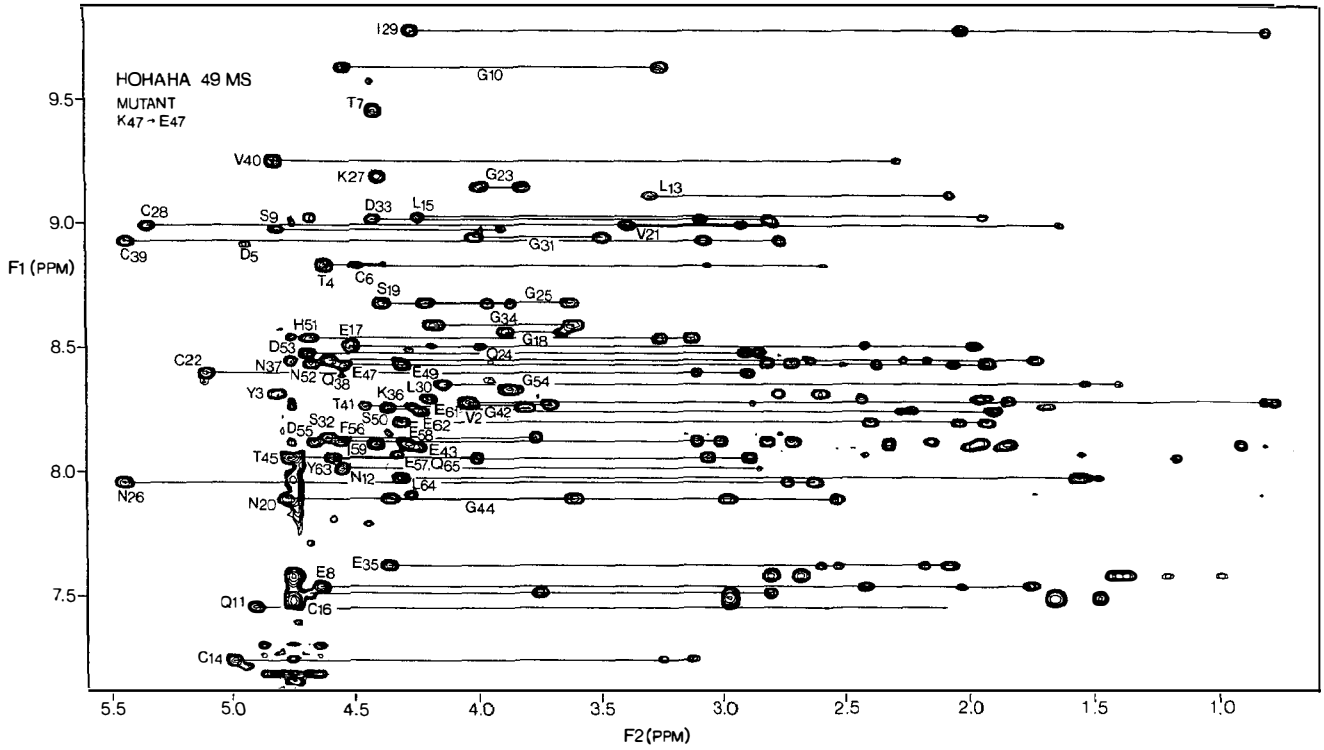

Figure 4 Part of a 600 MHz HOHAHA spectrum of a mutant of hirudin, recorded with a 49 ms mixing period and using a pulse scheme that avoids irradiation of the H_2O resonance (173). Reproduced from Folkers et al (78). Reprinted with permission from *Biochemistry*. Copyright 1989, American Chemical Society.

stantial number of long-range NOEs is also present, providing the crucial information about the backbone fold.

The pulse scheme of the NOESY experiment (Figure 2*c*) consists of three radiofrequency pulses (26, 27). The duration of the delay, t_1, between the first and the second pulse is again systematically incremented in successive experiments until a complete two-dimensional data set is obtained. The duration, τ_m, between the second and third pulse is kept constant and is generally referred to as the mixing period. For macromolecules, the rate of magnetization transfer between protons is proportional to $r^{-6}\tau_c$, where r is the interproton distance and τ_c is the molecular correlation time. For small proteins, τ_m is typically chosen between 50 and 200 ms. For the short mixing period, only relatively short interproton distances (shorter than about 3 to 3.5 Å) will give rise to observable correlations. For the longer mixing times, a much larger number of correlations can be observed, corresponding to distances up to 5 Å. In principle, because of the steep r^{-6} distance dependence of the magnetization transfer rate, one would expect that NMR permits very sensitive distance measurements. As will be discussed later, quantitation of the transfer rate and calculation of distances from such rates can be subject to serious errors. However, for sequence-specific assignments it suffices to use NOE cross peak intensities (NOEs) in a qualitative manner. Short distances ($<$ 2.5 Å) always yield substantial NOEs, medium-range distances (2.5–3.5 Å) yield weaker NOEs, whereas distances larger than 3.5 Å are often too weak to be observed in the short mixing time NOESY spectra.

Distances between backbone (CαH, NH) protons, and between a backbone and CβH protons on adjacent amino acids, are termed *sequential* distances. These strongly depend on the protein structure, i.e. on the intervening ϕ, ψ, and χ torsion angles (5, 55). For example, for an α-helix, the sequential NH-NH distance, d_{NN}, is about 2.8 Å, and the distance between CαH of residue i and the NH proton of residue $i + 1$ ($d_{\alpha N}$) is about 3.5 Å. In contrast, in β-sheets d_{NN} is about 4.2 Å, and $d_{\alpha N}$ is 2.2 Å. Wüthrich and coworkers have tabulated sequential backbone distances for all secondary structural elements, including turns of types I and II, and the recently proposed half turn (56). They concluded that in the sterically allowed region of ϕ and ψ angles of the Ramachandran plot, at least one sequential distance is always less than 3 Å. The possible types of sequential NOE connectivities are schematically indicated in Figure 5*a;* the sequential backbone NOE intensities for various types of secondary structure are schematically depicted in Figure 5*b*. For each amino acid, at least one and usually two sequential connectivities can be observed in high-quality NOESY spectra. Since some amino acids have unique spin system topologies, the scalar connectivity networks obtained with the COSY and HOHAHA experiments have made it possible to determine what type of amino acid corresponds to the NH, CαH, and CβH resonances. Sequential connectivity between two residues of known type then can provide

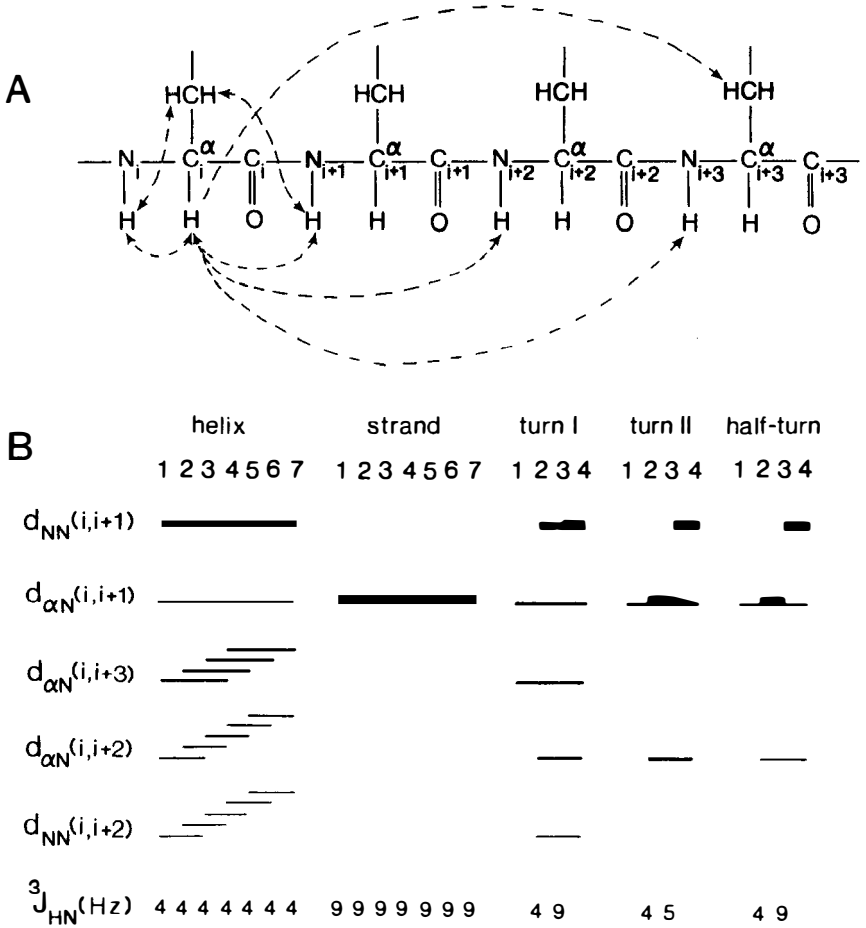

Figure 5 (*A*) Broken lines indicate some of the NOE interactions that may be observable in polypeptide chains. (*B*) NOE intensities and NH-CαH J couplings in several types of secondary structure. The thickness of the horizontal lines indicates the intensity of the NOEs.

an anchoring point in the sequence, provided that this dipeptide is unique in the known amino acid sequence of the protein. To avoid branching in a wrong direction, it is essential to have a large number of these unique dipeptides located along the protein backbone. If done carefully, the sequential assignment procedure can be applied to proteins of over 100 amino acids, as illustrated by a detailed example presented by Redfield & Dobson (57) for hen egg white lysozyme (129 residues).

At first sight, the procedure outlined above appears very straightforward. However, a requirement is that each NH and each CαH proton has its own unique chemical shift. On average, α-helixes show relatively little chemical

shift dispersion, whereas β-sheeted domains typically show much better dispersion of both NH and CαH protons. In practice, the resolution with which a peak position can be determined reliably is at best ± 0.01 ppm, and following this criterion, even for small proteins, less than half the residues have unique chemical shifts for both NH and CαH protons (58). Therefore, even while there may be little overlap in the 2D NMR spectrum, it becomes difficult to determine which correlation peak corresponds to which particular pair of protons. For example, two overlapping NH resonances may each show intraresidual and sequential NH-CαH connectivities, and it is then unclear which of the four cross peaks corresponds to which of the amide protons. One commonly used procedure to alleviate this serious problem is to record a set of 2D NMR spectra under slightly different experimental conditions. Particularly the NH protons are often quite sensitive to pH and temperature, and different residues shift differently with temperature and pH. In addition, non–hydrogen-bonded NH protons often rapidly exchange when the protein is dissolved in D_2O, simplifying the NH-CαH region. As many as half a dozen or more NOE spectra may therefore be needed to remove most ambiguities in the sequential assignment procedure. More sophisticated approaches for solving this overlap problem rely on labeling with stable isotopes and on three-dimensional NMR experiments, to be discussed later.

The two major types of secondary structure in proteins, α-helixes and β-sheets, show characteristic, easily recognizable fingerprints in the NOESY spectrum. α-helixes are characterized by a sequence of short sequential NH-NH connectivities, corresponding to the 2.8 Å interproton distance. As an example, Figure 6 shows the amide region of the 500 MHz NOESY spectrum of hen egg white lysozyme, with the sequential series of d_{NN} connectivities corresponding to one of the α-helixes marked. Intraresidue NH-CαH distances in α-helixes are also short (2.4 Å) and give rise to intense correlations too. In addition, weak interresidue correlations often can be observed between NH and the CαH of the preceding residue ($d_{\alpha N}$ connectivity) and to the CαH of the residue three positions earlier in the sequence ($d_{\alpha N}(i,i+3)$). Correlations between NH resonances and the Cβ protons of the preceding residue (dβN) are also commonly observed, as well as weaker $d_{\alpha N}(i,i+2)$ and $d_{\alpha N}(i,i+4)$ connectivities. Antiparallel β-sheets are characterized by intense CαH-CαH cross peaks for residues on opposite strands, in addition to an intense sequential $d_{\alpha N}$ connectivity. Parallel β sheets show the strong sequential $d_{\alpha N}$ connectivity, but only weak CαH-CαH cross peaks are observed.

Measurement of J Couplings

The J coupling between protons three bonds apart has a characteristic dependence on the dihedral angle, θ. This dependence is described by a so-called Karplus equation (59):

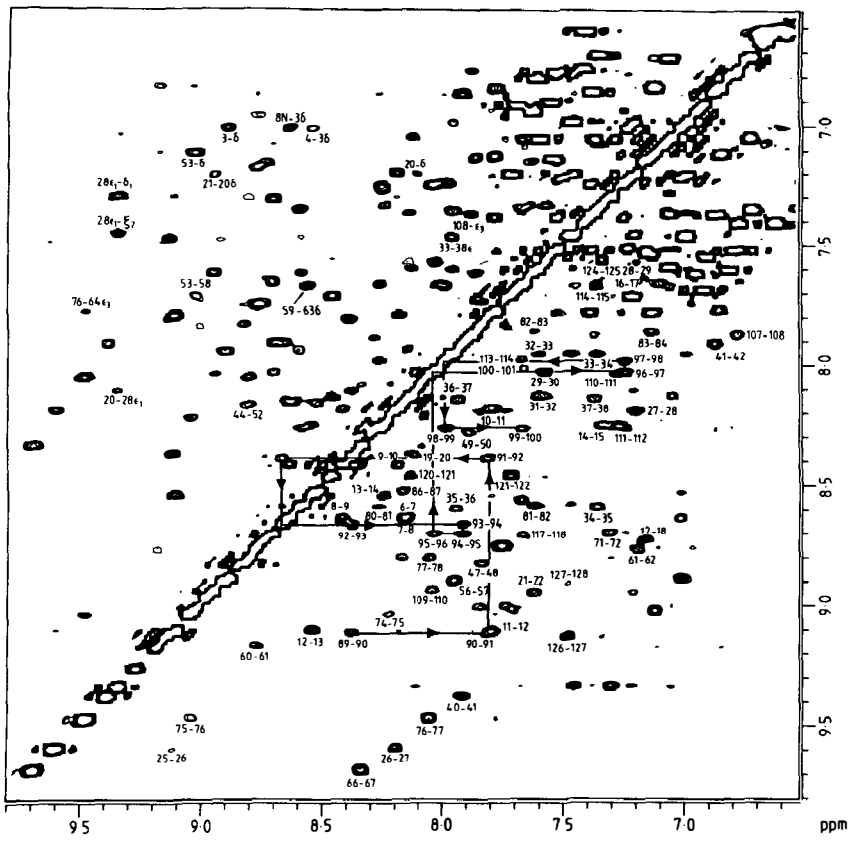

Figure 6 NH and aromatic region of the 500-MHz NOESY spectrum of hen lysozyme in H_2O, recorded with a 150-ms mixing time. Connectivities involving pairs of neighboring NH protons are labeled in the region below the diagonal. Long-range NH-NH connectivities and NH-aromatic connectivities are labeled in the region above the diagonal. The cross peaks corresponding to the α-helix from residues 89 to 101 are connected by drawn lines. From Redfield & Dobson (57). Reprinted with permission from *Biochemistry*. Copyright 1988, American Chemical Society.

$$J(\theta) = A\cos^2\theta - B\cos\theta + C \qquad 1.$$

where the constants A, B, and C have been determined empirically (60–65) and θ angles of 0 and 180° correspond respectively to *cis* and *trans* arrangements of the hydrogens. For the CαH-NH coupling, A, B, and C values of 6.4, 1.4, and 1.9 appear to give best agreement between the measured couplings and the X-ray structure of the basic pancreatic trypsin inhibitor (65). For CαH-CβH couplings, A = 9.5, B = 1.6, and C = 1.8 give good results (64).

Accurate measurement of J couplings in the overlapping one-dimensional spectrum of a protein can be very difficult. If a particular proton is coupled to only one other proton (e.g. NH in all but Gly residues), a measure for the size of the J coupling can be obtained from the antiphase multiplet structure of the cross peak in a COSY spectrum (43). It should be noted however, that the measured coupling can be a serious overestimate of the actual coupling if the line width is larger than the J coupling (66, 67). Therefore, it is important to record the 2D COSY spectrum with very high resolution in the F_2 dimension where one wishes to measure the coupling. Careful use of this procedure, including line shape analysis of the antiphase multiplet structure, showed excellent agreement between the measured J values and X-ray ϕ backbone angles in hen egg white lysozyme (68).

For measurement of χ_1 angles in residues that contain a single β hydrogen (Thr, Val, Ile), a similar procedure as described above for the ϕ angle can be employed, provided that the amide proton is exchanged for a deuteron. Couplings between CαH and β-methylene protons are more difficult to measure. In principle, measurement from a high-resolution COSY spectrum may be possible by comparison with simulated cross multiplet patterns (69). A more elegant approach uses a modified COSY experiment, such as the E-COSY (42) or PE-COSY (44, 68) method, which simplifies the cross peak multiplet structure. The measured coupling represents the time average (on the 100-ms time scale) of the actual J coupling. Therefore, interpretation of the measured coupling may be difficult because it is not always possible to distinguish whether a J value corresponds to a single dihedral angle or whether it represents a rapid averaging of J values from quite different dihedral angles. In cases where the protein does not exist in a single conformation, but rather as an equilibrium of rapidly interconverting conformers, the NOE and J coupling contain information about the time average of the distance to the power negative six, r^{-6}, and the time average of the J coupling, respectively. Both averaging processes are strongly nonlinearly dependent on geometry, and the presence of multiple conformations therefore often results in NOEs and J couplings that could not simultaneously be consistent with a single conformation (70).

Stereospecific Assignments of Methylene and Methyl Resonances

Until recently, usually no stereospecific assignments of β-methylene protons or of the methyl groups in leucine and valine residues were made. To keep the structure calculations simple, a distance measured to a methylene proton is therefore entered into the computer program as a distance to the geometric center between the two methylene protons; a 1 Å correction is added to the upper bound of the measured distance to correct for the difference in position

of the so-called "pseudo atom" relative to the true proton (71). Similarly, a distance to a methyl group of valine or leucine usually is entered as a distance to the geometric center of the methyl protons, after increasing the upper bound for the measured distance 2.4 Å. For the nondistinguishable C2H/C6H and C3H/C5H protons of rapidly reorienting Phe or Tyr rings, a 2 Å correction is used. Intraresidue corrections and corrections on short range distances in regions of known secondary structure can be chosen smaller (71–73).

The pseudo-atom description of magnetically indistinguishable nuclei (such as the three protons of a rapidly rotating methyl group) provides a simple means for entering distance information concerning these nuclei. Because the pseudo-atom approach involves the use of looser distance constraints, the local structure is less well defined compared to the case where distances could be measured to individual protons. Recently, a very interesting alternative method has been proposed that avoids the pseudo-atom approach. By relaxing the chirality constraints on prochiral centers in the structure determination program, it is possible to input the distances as measured and have the program figure out which of the prochiral protons is which (74, 75). This new approach appears very promising, and at present it is not clear whether any hidden pitfalls could be associated with this method.

Whenever stereospecific assignments of prochiral resonances can be made, this should give the most reliable and accurate distance information. As demonstrated for valyl methyl groups by Zuiderweg et al (76a) and for β-methylene sites by Hyberts et al (69), stereospecific assignments of these resonances may be possible. For example, for valine residues in an α-helix, for steric reasons the side chains have to be in the g^+ conformation, positioning the $C\gamma^1$ methyl group much closer to the valine NH proton than the $C\gamma^2H_3$ protons (76a). Provided that the χ_1 torsion angle is close to one of its standard conformers, stereospecific assignment for non–α-helical valines and for leucine and β-methylene protons often can also be determined by using a combination of J coupling and intraresidual NOE information (76a, 55). Unambiguous stereospecific assignments for all residues, including glycine, can be obtained by biosynthetic incorporation of stereospecifically deuterated amino acids in the protein (58, 76b).

Preliminary results obtained by a number of research groups indicate large improvements in defining the local protein conformation when stereospecific assignments are used (77, 78). At present it is still unclear what percentage of the possible stereospecific assignments can be determined in an average small protein. So far, it appears that in practice only about 50% of the possible stereospecific assignments can be made in an unambiguous manner. However, it is expected that further improvements in methodology could increase this number significantly.

Accuracy of NMR Distance Determination

The NOESY experiment measures the rate at which protons exchange their nuclear magnetization. The off-diagonal resonance at coordinates $(F_1,F_2)=(\Omega_A,\Omega_B)$ corresponds to magnetization transferred from proton A to proton B during the mixing period, τ_m, of the NOESY experiment (Figure 2*a*). The intensity of this off-diagonal resonance can be measured with an accuracy of about 10%. As mentioned earlier, the NOE buildup rate depends on r^{-6}, where r is the distance between the two protons; therefore, one might hope to determine very accurate distances (±1.5%) from the NMR measurement. There are two major reasons why such high accuracy cannot be obtained in practice: local internal motion within the protein and indirect or relayed NOE effects.

The rate, k, at which the NOE effect transfers magnetization from spin A to spin B is given by:

$$k = [34.2\tau_c/(1 + 4\omega^2\tau_c^2) - 5.7\tau_c] \times 10^{10}r^{-6} \qquad 2.$$

where ω is 2π times the ^{1}H resonance frequency (usually about 5×10^8). As can be seen from this equation, for $\omega\tau_c >> 1$, k increases linearly with τ_c. For τ_c values smaller than $1.1/\omega$, k changes sign, and consequently, cross peaks in NOESY spectra of small peptides are opposite in sign relative to the diagonal resonances. A protein usually cannot be described by a single correlation time, however. In particular, the long amino acid side chains are subject to rapid motions of considerable amplitude. This increased local motion reduces the NOE buildup rate k in macromolecules. Moreover, the interproton distance, r, is modulated by the local motion and the measured NOE buildup rate reflects $<r^{-3}>^2$ (fast local motion) or $<r^{-6}>$ (slow local motion) (70). A recent molecular dynamics study of the effect of picosecond motions in proteins indicates that the effects of distance fluctuations are largely compensated by angular fluctuations, and that NOE cross peak intensities in the presence of fast local motion in practice may be analyzed using a $<r^{-6}>$ model (79a).

A second problem in quantitating NOE buildup rates is caused by indirect NOE effects. Consider three protons, A, B, and C, arranged in a linear fashion, with interatomic distances r_{AB} = 2 Å, r_{AC} = 4 Å, and r_{BC} = 2 Å. Direct magnetization transfer from A to B is 64 times faster than from A to C. However, in the experimental scheme, as soon as magnetization has been transferred from A to B, it can be transferred on to C because of the strong BC NOE interaction. To avoid this indirect effect, it is necessary to work at very short mixing times, such that only a small fraction of A magnetization has transferred to B by the end of the mixing time. Under such conditions, only very short distances yield cross peaks with sufficient intensity for reliable

measurement. If the approximate macromolecular structure is known (as it may be for DNA oligomers), one may be able to calculate the severity of the indirect effects and correct the analysis of the NOE intensities (79, 80). For proteins, such procedures are less straightforward. However, as shown by Marion et al (81), if a global fold structure is available from the inaccurate NMR data, it is possible to refine such a structure by taking the indirect NOE contributions into account in a similar manner as proposed by Keepers & James for DNA (79b). In contrast to DNA, for proteins it does not appear essential to measure distances with very high accuracy for obtaining a high-resolution structure. Model calculations demonstrate that even with very loose distant constraints, it is possible to define the protein structure with high precision (75, 82–90). This is attributed to the fact that the polypeptide folds back on itself, providing long-range distant constraints that are absent in DNA.

Most commonly, the NOE "distances" are classified in three categories: 1.8–2.7, 1.8–3.3, and 1.8–5 Å, for example. This classification is somewhat arbitrary but functions quite well in practice. Intense NOE cross peaks in a NOESY spectrum recorded with a short mixing time (about 50 ms) are classified as 1.8–2.7 Å; the weak resonances in such a spectrum fall in the second category. Additional NOEs that show up at longer mixing times (e.g. 200 ms) may be due to indirect effects and are classified in the 1.8–5 Å group. The lower boundary is kept the same in each of these groups because local motion could severely attenuate the NOE, even for short distances. Computer simulations suggest that the use of much tighter constraints does not lead to a dramatic improvement in determination of the protein structure (86–88).

Determination of Tertiary Structure

Determination of the relative orientations of segments of secondary structure requires the use of so-called long-range NOEs between residues that are more than five residues apart in the sequence. In the first step of this process, long-range NOE cross peaks between two protons can only be used if both protons have unique chemical shifts, i.e. are at least 0.01 ppm removed from any other proton. Usually, relatively few of such NOEs can be found in a typical NOESY spectrum of a protein. However, even with few long-range NOE contacts, it is possible to obtain some idea about the relative orientations of individual domains. From the low-resolution structure thus obtained, it then becomes possible to assign a larger number of long-range NOEs, permitting the generation of a more accurate structure, which may permit additional long-range NOEs to be identified.

The crude structure mentioned above may be obtained by manual model building or by using molecular graphics. However, this type of structure is very qualitative and more work is needed to find the structure that best fits the

NMR data, without violating any of the standard geometrical constraints, such as bond angles, bond lengths, and van der Waals radii. Most commonly used are two approaches, the so-called distance geometry approach and restrained molecular dynamics. The merits of each of these methods for NMR structure determination have been discussed in a number of places (13, 73, 75, 82–90), and only a very brief discussion of this essential step of the structure determination process is presented here.

Distance geometry is a mathematical tool that can be used to obtain protein structures that satisfy internuclear distances determined with NMR. This type of mathematical problem has been addressed long before interproton distances in proteins could be measured (91), but recent developments in protein NMR have provided a new impetus for further perfection of such procedures, in particular with respect to speed and the necessity to handle large arrays of data. Also, efficient algorithms had to be developed to overcome one of the major difficulties in using distance geometry: the problem of local minima. Of the large variety of algorithms suitable for determination of protein structure from NMR data (86, 88, 92–97), two quite different distance geometry programs now appear to be most widely used: DISGEO (86) and DISMAN (88). The DISMAN program does not work in distance space and therefore it is not a true distance geometry technique; instead, it relies on minimization in torsion angle space rather than Cartesian space. DISMAN uses a so-called variable target function. First, only NMR constraints between residues that are close in the polypeptide sequence determine the local folding; distances further and further apart in the sequence are then gradually incorporated in the target function. The DISGEO program uses n-dimensional space to overcome the local minimum problem. A detailed comparison of the two programs demonstrates that both are capable of faithfully reproducing a protein structure from NMR data (89). The root-mean-square deviation (RMSD) of a set of NMR structures, calculated from the same set of data but using randomly selected starting conditions, is often used to assess the quality of the NMR structure. In this respect, it was found that the RMSDs for the DISGEO tend to be smaller than for DISMAN. However, comparison of the DISMAN and DISGEO structures with the original crystal structure from which the artificial NMR constraints were derived, showed that the difference in RMSD was largely caused by the fact that in regions of the protein that are relatively poorly constrained by NMR data, the DISGEO program tends to produce slightly expanded structures, insufficiently reflecting the lack of NMR constraints. Better agreement between the calculated structure and NMR data and a lowering of the computed energy of the protein can be obtained by subjecting the distance geometry structure to a restrained molecular dynamics simulation (48), to be discussed below.

Restrained molecular dynamics (RMD) is a conceptually relatively simple

alternative to distance geometry algorithms. It uses a modification of the regular molecular dynamics simulation programs (98–101). Restrained molecular dynamics solves Newton's equations of motion, with the potential energy, V, defined by:

$$V = V_{bond} + V_{vdW} + V_{angle} + V_{dihedr} + V_{coulomb} + V_{NMR} \qquad 3.$$

where V_{bond}, V_{angle}, and V_{dihedr} keep bond lengths, angles, and chirality at their equilibrium values. The van der Waals and electrostatic interactions are described by V_{vdW} and $V_{coulomb}$. V_{NMR} contains the NMR constraints; it has the effect of pulling the protons that show an NOE interaction closer to the measured distance, r_{ij}. Similarly, V_{NMR} may also contain J-coupling information by including a torsion term. Restrained molecular dynamics was first applied to the NMR structure determination problem by Kaptein et al (102) and Clore et al (103). Although, in principle, an arbitrary starting structure may be used for the restrained molecular dynamics calculation (82), in practice a starting structure obtained by means of distance geometry algorithms (13, 104, 105) or by model building is often used (102, 106). Because of the kinetic energy present in the protein during the dynamics simulation, this procedure can be efficient at overcoming the problem of local minima. The RMD approach requires a relatively large amount of computational time compared to the distance geometry methods. This problem can be overcome by using a simplified potential energy function, where all nonbonded contact interactions are described by a single term. By using a lower cutoff distance, the number of nonbonded interactions is also decreased significantly. This process, referred to as simulated annealing (107), is computationally more efficient than RMD and yields structures of similar quality (75, 85). A combined use of the first stages of the DISGEO structure calculation procedure followed by simulated annealing appears to be an extremely fast structure calculation method, capable of providing high-quality structures (108).

For experimental data, one typically uses a large number (20 to 100) of different starting structures (or starting distances for DISGEO) for the DG or MD algorithms. If a significant fraction of the thus calculated structures satisfies all NMR constraints, and shows small root-mean-square (RMS) deviations from one another (<2 Å for all backbone atoms), this indicates that the calculated structures must be close to the actual solution structure. If serious violations of NMR constraints remain, or if the RMS deviation between the various structures is too large, reanalysis of the NMR spectra is necessary. Another useful indication of the agreement between the NMR data and the molecular structure can be obtained if an NOE spectrum is calculated from the obtained protein structure. Comparison of the real and the calculated

NOE spectra gives a visual impression of the agreement between the experimental NMR spectrum and the protein structure (55, 81).

Quality of NMR Structures

Until recently, NMR protein structures were determined at a low level of detail, showing the global backbone fold typically with RMS deviations of at least 1.5 to 2 Å. The definition of side chains, if presented at all, was significantly poorer. More recently, with the use of stereospecific assignments and the availability of stronger magnetic fields, this situation appears to be changing, although to date very few "high-resolution" NMR protein structures have actually been published (77, 78, 89, 130). Nevertheless, even at relatively low resolution, a comparison of structural features in solution and in the crystalline state is possible, as briefly discussed below.

NMR structures have been determined for a number of proteins for which a high-resolution crystal structure was already available. Proteins for which good agreement between the two types of structure is found include BPTI, potato carboxypeptidase inhibitor (CPI) (105), and barley serine proteinase inhibitor 2 (BSPI-2) (109). For BPTI, minor differences are found at the surface of the protein (89). For CPI, small deviations from the crystal structure were reported for two regions of the backbone (105). For BSPI-2, the small RMS difference (1.9 Å) for the backbone atom positions between crystal and solution structure appears not to be localized in particular regions of the protein (110).

For epidermal growth factor (EGF) no crystal structure was available, but three groups independently determined very similar structures for the two domains of this polypeptide (111–115) despite significant differences in the quality of the NMR data available to them. The Japanese group (112, 113) found a different relative orientation of the two domains, but this may be due to different conditions under which the spectra were recorded, and it is not certain the two domains have a fixed relative geometry under all conditions.

A few significant differences between NMR and X-ray structures have also surfaced recently. Most interesting, two-dimensional ^{1}H-^{113}Cd correlation experiments (116–118) revealed that the cadmium coordination in the solution and crystal structure (119, 120) of metallothionein-2a is quite different (116). At present, it is unclear whether this is due to a problem in the X-ray refinement procedure, or to crystallization of a minor component of the protein. Differences between the crystal structure and the solution data have been reported by Nettesheim et al (121) for the human complement protein C3A. These authors attributed the substantial differences in helical structure, observed both at the C and N termini, to crystal packing forces.

Discrepancies between the X-ray crystal structure and NMR data of α-bungarotoxin were reported by Inagaki et al (122). A recent detailed NMR

structural study by Basus et al (123) confirmed a different orientation of Trp-28, and showed the presence of a more extended β-sheet structure in solution, making it more similar to the homologous cobratoxin crystal structure. This NMR study also identified four errors in the primary sequence of the protein. These errors had remained undetected in the 2.5 Å crystal structure (124). Other incorrect primary sequences were detected for metallothionein-2a from rabbit liver (56), protease inhibitor IIA from bull seminal plasma (125a, 125b), and for toxin II from *Radianthus paumotensis* (126).

The structure of the α-amylase inhibitor, Tendamistat (74 amino acids) was determined simultaneously and independently by the crystallographic group of Huber (127) and by Kline, Braun, and Wüthrich (129, 130). The backbone folds of the solution and crystal structures were virtually identical, although small differences in some of the side chain conformations were observed between the two structures. The NMR structure had been obtained using a very large number (842) of NOEs and many stereospecific assignments and dihedral constraints from J couplings, and the solution structure is of much higher quality than most NMR structures. RMS deviations between the NMR structures were 0.85 Å for the backbone, 1.04 Å for the backbone plus the interior amino acid side chains, and 1.53 Å for all heavy atoms. The differences between the solution and crystal structures were 1.0, 1.3, and 1.8 Å, respectively.

Solution structures of two other small proteins with similarly high resolution, also using stereospecific assignments and dihedral constraints, have recently been derived by Driscoll et al (77) and by Folkers et al (78). As an example, Figure 7 shows a superposition of 42 structures obtained for the antihypertensive and antiviral protein BDS-I from the sea anemone *Anemonia sulcata*. The high degree of similarity of the 42 structures reflects the large number ($>$ 500) of NOE and dihedral constraints used for this small protein (46 amino acids).

PROSPECTS FOR THE STRUCTURE DETERMINATION OF LARGER PROTEINS

The NMR study of proteins significantly larger than 10 kd is hampered by a number of factors. Most importantly, the molecular correlation time increases nearly linearly with molecular weight and leads to a significant increase in line width. This not only increases crowding in the 2D NMR spectra, it also reduces sensitivity, particularly for the essential J correlation methods (32–45). The molar concentrations of nonaggregating protein, on average, decrease with increasing molecular weight, lowering NMR sensitivity even further.

One important approach, to be discussed below, for obtaining detailed

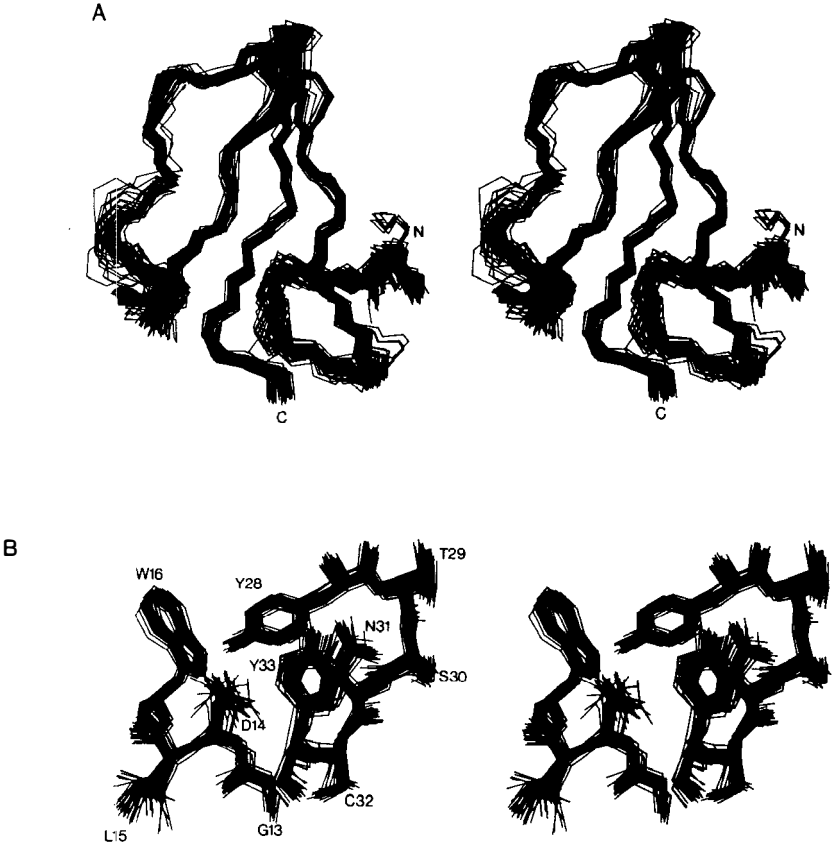

Figure 7 Stereoviews of the solution structure of the protein BDS-I from the sea anemone *Anemonia sulcata*. (*A*) superposition of 42 backbone structures and (*B*) all atoms of residues 13–16 and 28–33. The structures have been calculated with the simulated annealing procedure; 42 out of 50 calculated structures showed correct stereochemistry and no distance violations larger than 0.5 Å. From Driscoll et al (77). Reprinted with permission from *Biochemistry*. Copyright 1989, American Chemical Society.

NMR structural information relies on the incorporation of stable isotopes (^{15}N, ^{13}C, ^{2}H) in the protein. However, it should be noted that for a number of proteins larger than 10 kd virtually complete resonance assignments have been reported without the use of isotopic labeling. These include plastocyanin (131a–c), *Escherichia coli* thioredoxin (132), hen egg white lysozyme (57), and acylphosphatase (133). These proteins all are relatively "NMR friendly," showing good resonance dispersion and permitting the use of relatively high protein concentrations without significant aggregation.

For proteins that are genetically expressed in microorganisms, incorpora-

tion of stable isotopes can be relatively easy, and permits use of alternative methods for obtaining structural and assignment information. Random labeling with ^{15}N, ^{13}C, or ^{2}H can be achieved by feeding the microorganism with labeled precursors, such as $^{15}NH_4Cl$, ^{13}C-succinate, $^{2}H_2O$, and ^{2}H-glucose. For some experiments, to be discussed below, it is beneficial to label only certain types of amino acids. This can be accomplished by feeding with suitably labeled amino acid precursors. For efficient incorporation, the use of auxotrophic strains of the microorganism may be required (134). In the case of ^{15}N labeling, transaminase activity must be reduced by flooding the cells with excess of unlabeled amino acids (135) or by genetic modification (136). In cases where the expression occurs very rapidly (less than one hour), use of auxotrophic strains may not be essential, although scrambling among certain types of amino acids can then be expected (137). Two-dimensional isotope labeled NMR has recently been reviewed by Griffey & Redfield (138).

Double Labeling with ^{13}C and ^{15}N

One particularly powerful method for obtaining sequence-specific assignments relies on the use of double labeling; one type of amino acid (for example, Met) is labeled with ^{15}N and another type of amino acid (for example, Leu) is labeled with ^{13}C in its carbonyl position. As first demonstrated by Kainoshi & Tsuji (139), this approach permits immediate identification of the Leu-Met dipeptide because the carbonyl resonance of the Leu prior to the Met residue shows a J splitting caused by interaction with the ^{15}N nucleus. A powerful and very sensitive extension of this technique does not detect the ^{13}C signal, but uses the more intense ^{1}H signal to detect the attached ^{15}N nucleus in a two-dimensional experiment (140–143). ^{15}N nuclei adjacent to ^{13}C will show the J splitting in the ^{15}N dimension of the 2D spectrum, identifying the dipeptide (144). Figure 8 shows two such correlation spectra, obtained for staphylococcal nuclease (18 kd) doubly labeled with ^{15}N Met and $^{13}C'$ Leu or $^{13}C'$ Lys.

^{2}H Labeling

The ^{1}H line width problem can be overcome by incorporating deuterium, which dilutes the ^{1}H density in the protein and therefore reduces dipolar broadening (145, 146). Deuterium has a seven times smaller magnetogyric ratio compared to protons, and consequently its dipolar broadening effect on remaining protons is quite small. This effect has been demonstrated most dramatically by LeMaster & Richards (58) in a study of thioredoxin with random deuteration of the nonexchangeable protons. As they pointed out, the loss in concentration of hydrogens is compensated in part by the resulting narrower line widths. A substantial gain in sensitivity is observed in the NH-NH region of the NOE spectrum because no dilution of these exchangeable resonances occurs, and because during the mixing period of the NOESY

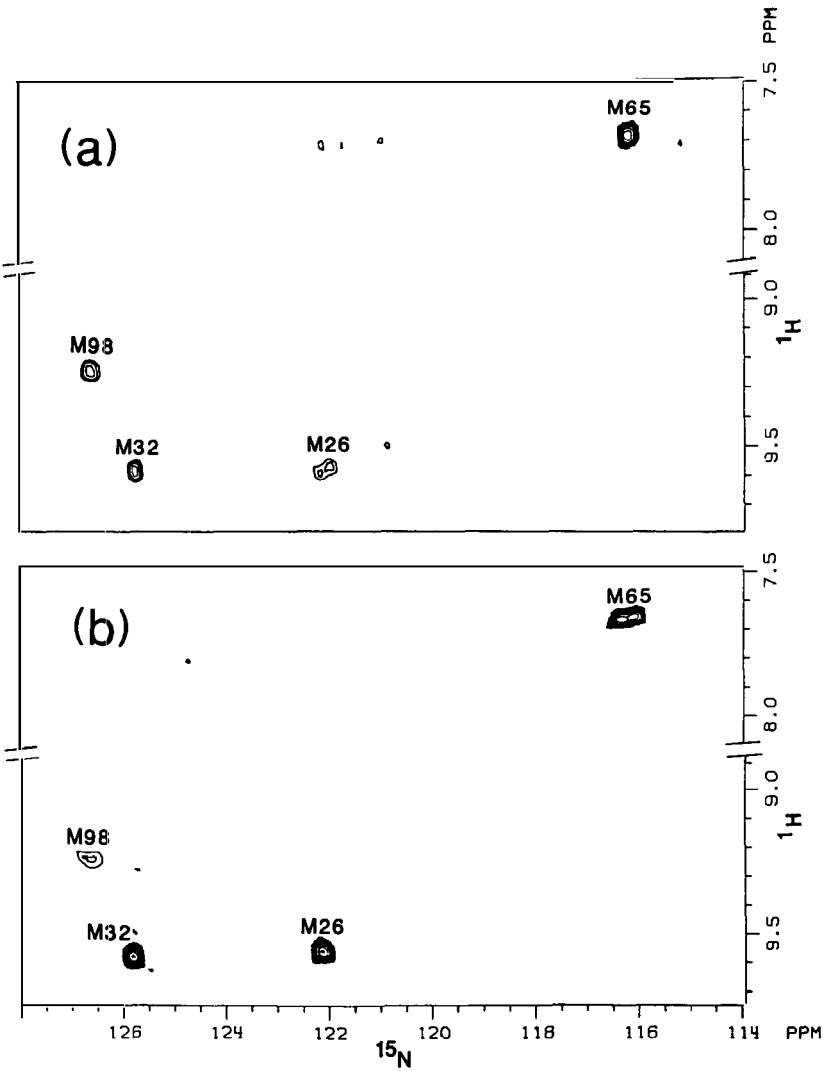

Figure 8 Comparison of ^{1}H-^{15}N shift correlation spectra of 1.5 mM staphylococcal nuclease in 90% H_2O/10% D_2O, labeled with (*a*) [1-^{13}C]Leu and [^{15}N]Met and (*b*) [1-^{13}C]Lys and [^{15}N]Met. Met-26 is preceded by a leucine residue and shows a splitting caused by the carbonyl-nitrogen J coupling. Similarly, Met-65 and Met-98 are preceded by lysine residues and show J splittings. From Torchia et al (137).

experiment these resonances lose less magnetization to (deuterated) aliphatic side chains (58, 147). An example in the increase in multiplet resolution observed upon 75% deuteration is shown in Figure 9. The possibility to deuterate stereospecifically (58) is also expected to be important for the study of medium-size proteins. Furthermore, the old idea (145) of incorporating

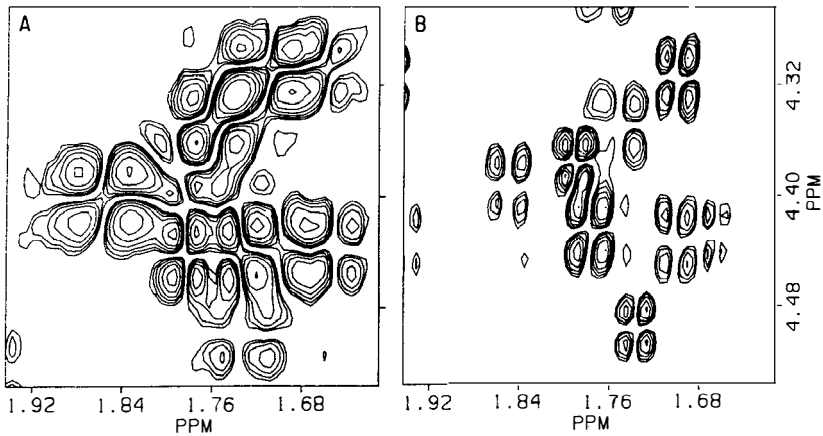

Figure 9 Comparison of small regions of the COSY spectra of *E. coli* thioredoxin. Panel A is recorded for a natural abundance sample, and panel B is the corresponding region for the 75% uniformly ^{2}H-labeled sample. The improved resolution observed for the fractionally deuterated sample is partly due to the longer T_2 relaxation time and hence narrower line width, but mainly is a result of the fact that coupling from other protons to the two protons involved in the coherence transfer is largely eliminated by the isotopic dilution. From LeMaster & Richards (58). Reprinted with permission from *Biochemistry*. Copyright 1988, American Chemical Society.

certain protonated amino acids into an otherwise fully deuterated protein offers interesting possibilities for spectral simplification and resonance assignment (137).

Isotope-Edited Experiments

It is relatively straightforward to exclusively observe hydrogens that are directly attached to either ^{15}N or ^{13}C (148). As demonstrated by a number of research groups (149–153), it is then relatively straightforward to incorporate this editing procedure into two-dimensional experiments, greatly simplifying the corresponding spectra. These edited 2D spectra thus can show a great reduction in spectral crowding, as demonstrated in Figure 10. However, it should be noted that for experiments involving incorporation of ^{13}C, the strong heteronuclear dipolar ^{13}C-^{1}H interaction causes significant extra broadening of the ^{1}H resonances, making this type of editing approach less suitable for J-correlated 2D experiments. Complete ^{15}N labeling of proteins offers another possibility for spectral simplification of the amide region: by labeling in the F_1 dimension with the ^{15}N chemical shift instead of the amide ^{1}H shift, many degeneracies present in the regular NOESY spectrum can be removed, facilitating sequential assignment (154).

^{13}C and ^{15}N Experiments

The sensitivity of ^{13}C and ^{15}N NMR spectra of proteins at natural abundance is too low for permitting advanced 2D NMR experiments of proteins of a

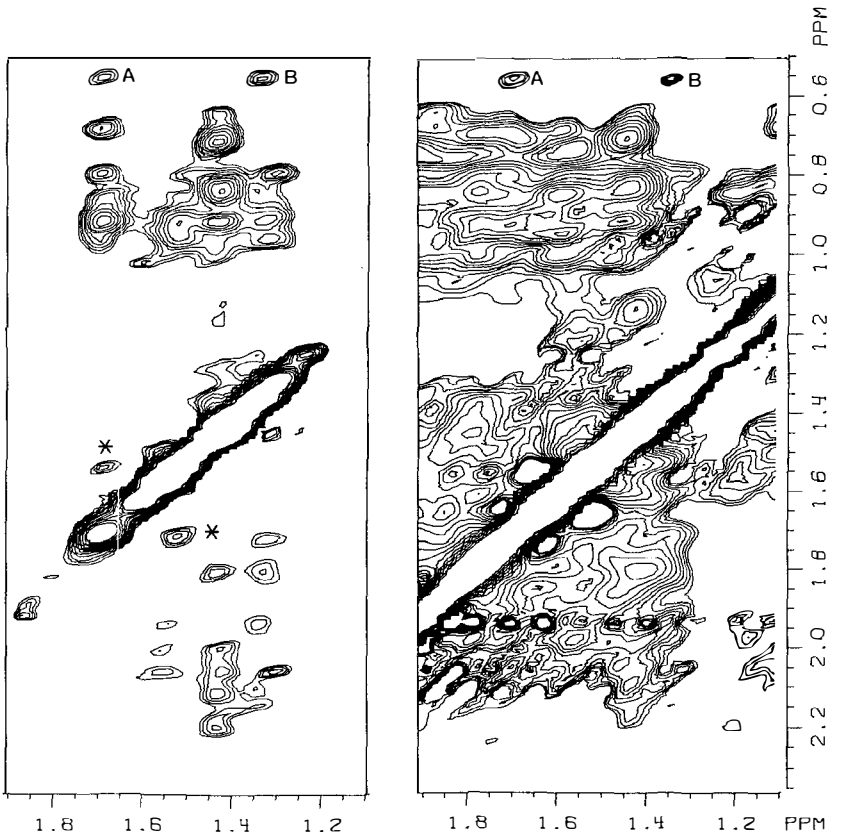

Figure 10 Comparison of small regions of the NOESY spectra of [$^{13}C\beta$]Ala lambda repressor. The left panel shows the result of NOE editing and exhibits interactions only to ^{13}C-labeled protons, i.e. to the alanine methyl groups. The right panel shows the identical region of the conventional NOESY spectrum. Both spectra were recorded with a 300 ms NOE mixing time. From Bax & Weiss (149). Reprinted with permission from the *Journal of Magnetic Resonance*. Copyright 1987, Academic.

significant size. However, as convincingly demonstrated by Markley and coworkers (155, 156), when isotopic enrichment is used in combination with large sample volumes, a number of very powerful experiments become feasible. For example, using uniform labeling with ^{13}C permits detection of J connectivities between adjacent carbons (156). Because ^{13}C has a significantly larger spread in chemical shifts than ^{1}H, spectral crowding may be reduced. Moreover, ^{13}C chemical shifts for a certain type of carbon in a particular amino acid are quite predictable, facilitating spectral assignment. Sequential connectivity determination becomes possible when the protein is also labeled with ^{15}N, and ^{13}C–^{15}N 2D correlation experiments are performed (157). Once

complete ^{13}C assignments have been obtained, other 2D NMR experiments (140–143) can be used for correlating the ^{13}C resonances with chemical shifts of their directly attached protons (158, 159). J correlation through multiple bond ^{1}H-^{13}C or ^{1}H-^{15}N is often also possible, providing assignment and structural information (159–161).

Three-Dimensional NMR

For small proteins, the overlap present in one-dimensional NMR is largely removed in 2D NMR spectra. In a similar fashion, overlap present in the 2D spectra of larger proteins can be removed by extending the experiment to three dimensions (162–164). The first protein experiments have concentrated on combining the NOESY and HOHAHA pulse schemes, yielding spectra that display J connectivity in one plane and NOE connectivity in a perpendicular plane (165, 166). The final 3D spectrum contains a very large number of resonances, and interpretation of the entire information content at present is a formidable task. Software, currently under development in a number of laboratories, will greatly simplify the interpretation process and permit full utilization of this type of 3D experiment. A drawback of this particular 3D experiment is that there are two magnetization transfer steps involved: one NOE step and one HOHAHA mixing period. The efficiency of the HOHAHA step, which depends on the J coupling and is attenuated by increased line width, rapidly decreases for increasing molecular weight. Therefore, it is not certain at present whether this particular 3D experiment will be useful for the study of proteins significantly larger than 10 kd.

A more promising experiment, in this respect, combines heteronuclear chemical shift correlation with the regular NOESY experiment (167). By using uniform ^{15}N labeling of the protein, it is possible to separate the part of the regular NOE spectrum that shows interactions with amide protons according to the ^{15}N chemical shift. The number of resonances in such a spectrum is identical to the number of resonances in the regular NOE spectrum and sensitivity is very similar. However, spectral overlap is almost completely removed in the 3D spectrum. An example of a slice taken through a 3D spectrum of the protein staphylococcal nuclease is shown in Figure 11. Measurement time for 3D spectra is necessarily longer than for 2D spectra and can require up to several weeks of precious instrument time. However, the large amount of information present in such spectra may make this approach the method of choice for problems too complicated to be handled by conventional 2D NMR experiments.

DISCUSSION

NMR structural studies are not limited to aqueous solutions. Studies of the membrane-active peptides, melittin and glucagon, have been conducted in

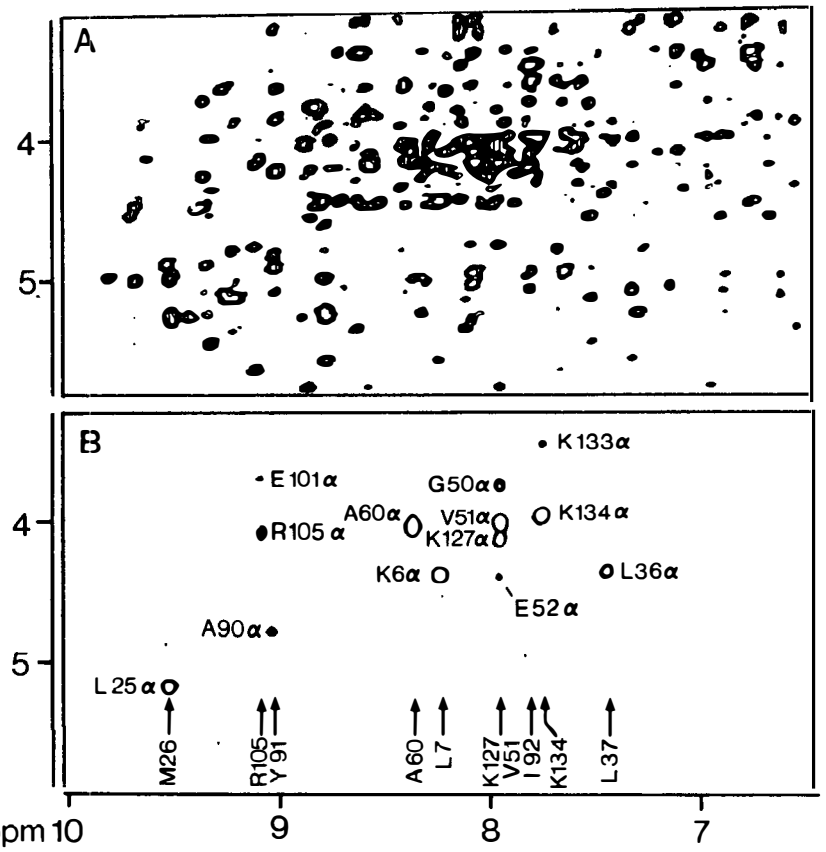

Figure 11 NH-CαH NOE interactions observed for a 1.5 mM sample of ^{15}N-labeled staphylococcal nuclease in 90% H_2O, using a 125 ms NOE mixing time. Panel A corresponds to the regular 2D NOESY spectrum; panel B is the corresponding region taken from a three-dimensional NMR spectrum where the NOESY spectra are separated according to the ^{15}N chemical shift of the amide nitrogen. The section shown displays NH-CαH correlations only for those amides that have a ^{15}N chemical shift of 122.3 ± 0.3 ppm. Adapted from Marion et al (172).

micelles, indicating conformations significantly different from either solution or crystal structures (168, 169). A study of filamentous bacteriophage coat protein in micelles yielded interesting information about both structure and dynamics of this polypeptide (170).

Even among crystallographers skepticism seems to be disappearing about the possibility of using NMR to determine solution structures of small proteins. At present, solution structures of nearly 50 small proteins or protein domains have been published or are in the process of being published. Continuing rapid developments in NMR methodology and equipment are extending the size limits of proteins under NMR investigation. Already, a

low-resolution NMR structure has been obtained for the *lac* repressor headpiece interacting with its operator (171). Similar studies for the *cro* and *lambda* repressor-operator complexes are under way. For suitable small proteins, the structure can sometimes be determined very fast, in less than a few months. However, the time and the amount of work needed for larger molecules rapidly increases. Most likely, therefore, even in the distant future, detailed NMR structural studies will largely remain limited to relatively small proteins or protein domains ($<$ 40 kd).

NMR structures, even at relatively low resolution, offer valuable complementary information to X-ray crystallography. NMR may become particularly useful for characterization of protein surfaces. In addition, NMR can probe motions over a time scale spanning 10 orders of magnitude and can provide significant insights in problems regarding protein folding and dynamics.

ACKNOWLEDGMENTS

I thank Ted Becker, Marius Clore, Angela Gronenborn, Lewis Kay, David LeMaster, Dominique Marion, Dennis Torchia, and Attila Szabo for stimulating discussions and useful comments and Ingrid Pufahl for assistance during the preparation of this manuscript.

Literature Cited

1. Jeener, J. 1971. Ampere International Summer School. Basko Polje, Yugoslavia
2. Wagner, G., Wüthrich, K. 1982. *J. Mol. Biol.* 155:347–66
3. Wagner, G., Wüthrich, K. 1982. *J. Mol. Biol.* 160:343–61
4. Kumar, A., Wagner, G., Ernst, R. R., Wüthrich, K. 1980. *Biochem. Biophys. Res. Commun.* 95:1–6
5. Billeter, M., Braun, W., Wüthrich, K. 1982. *J. Mol. Biol.* 155:321–46
6. Wüthrich, K., Wider, G., Wagner, G., Braun, W. 1982. *J. Mol. Biol.* 155:311–20
7. Wider, G., Lee, K. H., Wüthrich, K. 1982. *J. Mol. Biol.* 155:367–88
8. Wüthrich, K., Billeter, M., Braun, W. 1984. *J. Mol. Biol.* 180:715–40
9. Wagner, G. 1983. *Q. Rev. Biophys.* 16:1–57
10. Wüthrich, K. 1986. *NMR of Proteins and Nucleic Acids*. New York: Wiley
11. Wemmer, D. E., Reid, B. R. 1985. *Annu. Rev. Phys. Chem.* 36:105–37
12. Clore, G. M., Gronenborn, A. M. 1987. *Protein Eng.* 1:275–88
13. Kaptein, R., Boelens, R., Scheek, R. M., van Gunsteren, W. F. 1988. *Biochemistry* 27:5389–95
14. Bax, A. 1982. *Two-dimensional Nuclear Magnetic Resonance*. Boston: Reidel
15. Ernst, R. R., Bodenhausen, G., Wokaun, A. 1987. *Principles of Nuclear Magnetic Resonance in One and Two Dimensions*. Oxford: Clarendon
16. Chandrakumar, N., Subramanian, S. 1987. *Modern Techniques in High Resolution FT NMR*. New York: Springer
17. Croasmun, W. R., Carlson, R. M. K., eds. 1987. *Two-dimensional NMR Spectroscopy*. New York: VCH
18. Sanders, J. K. M., Hunter, B. K. 1987. *Modern NMR Spectroscopy*. Oxford: Univ. Press
19. Derome, A. E. 1987. *Modern NMR Techniques for Chemistry Research*. Oxford: Pergamon
20. Morris, G. A. 1986. *Magn. Reson. Chem.* 24:371–403
21. Benn, R., Günther, H. 1983. *Angew. Chem. Int. Ed. Engl.* 22:350–80
22. Kessler, H., Gehrke, M., Griesinger, C. 1988. *Angew. Chem. Int. Ed. Engl.* 27:490–536

23a. Ramsey, N. F. 1952. *Phys. Rev.* 86:243–57
23b. Emsley, J. W., Feeney, J., Sutcliffe, L. H. 1965. *High Resolution Nuclear*

Magnetic Resonance Spectroscopy, Vol. 1, pp. 65–103. Oxford: Pergamon
24a. Pardi, A., Wagner, G., Wüthrich, K. 1983. *Eur. J. Biochem.* 137:445–54
24b. Gross, K. H., Kalbitzer, H. R. 1988. *J. Magn. Reson.* 76:87–99
25. Noggle, J. H., Schirmer, R. H. 1971. *The Nuclear Overhauser Effect. Chemical Applications*. New York: Academic
26. Jeener, J., Meier, B. H., Bachmann, P., Ernst, R. R. 1979. *J. Chem. Phys.* 71:4546–53
27. Macura, S., Ernst, R. R. 1980. *Mol. Phys.* 41:95–117
28. Englander, S. W., Kallenbach, N. R. 1984. *Q. Rev. Biophys.* 16:521–655
29. Tuchsen, E., Woodward, C. 1985. *J. Mol. Biol.* 185:405–19
30. Billeter, M., Braun, W., Wüthrich, K. 1982. *J. Mol. Biol.* 155:321–46
31. Englander, S. W., Wand, A. J. 1987. *Biochemistry* 26:5953–58
32. Aue, W. P., Bartholdi, E., Ernst, R. R. 1976. *J. Chem. Phys.* 64:2229–46
33. Bax, A., Freeman, R. 1981. *J. Magn. Reson.* 44:542–61
34. Nagayama, K., Kumar, A., Wüthrich, K., Ernst, R. R. 1980. *J. Magn. Reson.* 40:321–34
35. Eich, G., Bodenhausen, G., Ernst, R. R. 1982. *J. Am. Chem. Soc.* 104:3731–32
36. Bax, A., Drobny, G. 1985. *J. Magn. Reson.* 61:306–20
37. Braunschweiler, L., Ernst, R. R. 1983. *J. Magn. Reson.* 53:521–28
38. Bax, A., Davis, D. G. 1985. *J. Magn. Reson.* 65:355–60
39. Rance, M. 1987. *J. Magn. Reson.* 74:557–64
40. Griesinger, C., Otting, G., Wüthrich, K., Ernst, R. R. 1988. *J. Am. Chem. Soc.* In press
41. Piantini, U., Sørensen, O. W., Ernst, R. R. 1982. *J. Am. Chem. Soc.* 104:6800–1
42. Griesinger, C., Sørensen, O. W., Ernst, R. R. 1985. *J. Am. Chem. Soc.* 107:6394–96
43. Marion, D., Wüthrich, K. 1983. *Biochem. Biophys. Res. Commun.* 113:967–74
44. Mueller, L. 1987. *J. Magn. Reson.* 72:191–96
45. Marion, D., Bax, A. 1988. *J. Magn. Reson.* In press
46. Zasloff, M. 1987. *Proc. Natl. Acad. Sci. USA* 874:5449–53
47. Clore, G. M., Martin, S. R., Gronenborn, A. M. 1986. *J. Mol. Biol.* 191:553–61
48. Clore, G. M., Sukumaran, D. K., Nilges, M., Gronenborn, A. M. 1987. *Biochemistry* 26:1732–45
49. Shaka, A. J., Freeman, R. 1983. *J. Magn. Reson.* 51:169–73
50. Boyd, J., Dobson, C. M., Redfield, C. 1985. *FEBS Lett.* 186:35–40
51. Müller, N., Ernst, R. R., Wüthrich, K. 1986. *J. Am. Chem. Soc.* 108:6482–92
52. Boyd, J., Redfield, C. 1986. *J. Magn. Reson.* 68:67–84
53. Rance, M., Wright, P. E. 1986. *J. Magn. Reson.* 66:372–78
54. Zuiderweg, E. R. P., Mollison, K. W., Henkin, J., Carter, G. W. 1988. *Biochemistry* 27:3568–80
55. Arseniev, A., Schultze, P., Wörgötter, E., Braun, W., Wagner, G., et al. 1988. *J. Mol. Biol.* 201:637–57
56. Wagner, G., Neuhaus, D., Wörgötter, E., Vasak, M., Kägi, J. H. R., Wüthrich, K. 1986. *J. Mol. Biol.* 187:131–35
57. Redfield, C., Dobson, C. M. 1988. *Biochemistry* 27:122–36
58. LeMaster, D. M., Richards, F. M. 1988. *Biochemistry* 27:142–50
59. Karplus, M. 1963. *J. Am. Chem. Soc.* 85:2870–71
60. Ramachandran, G. N., Chandrasekaran, R., Kopple, K. D. 1971. *Biopolymers* 10:2113–31
61. Cung, M. T., Marrand, M., Neel, J. 1974. *Macromolecules* 7:606–13
62. Bystrov, V. F. 1976. *Prog. Nucl. Magn. Reson. Spectrosc.* 10:41–81
63. Feeney, J. 1975. *Proc. R. Soc. London Ser. A* 345:61–72
64. DeMarco, A., Llinas, M., Wüthrich, K. 1978. *Biopolymers* 17:637–50
65. Pardi, A., Billeter, M., Wüthrich, K. 1984. *J. Mol. Biol.* 180:741–51
66. Neuhaus, D., Wagner, G., Vasak, M., Kägi, J. H. R., Wüthrich, K. 1985. *Eur. J. Biochem.* 151:257–73
67. Bax, A., Lerner, L. 1988. *J. Magn. Reson.* 79:429–38
68. Blazer, J., Dobson, C. M., Redfield, C. 1988. Abstr. #P15-24. *XIII ICMRBS Conf., Madison, Wis.*
69. Hyberts, S. G., Märki, W., Wagner, G. 1987. *Eur. J. Biochem.* 164:625–35
70. Kessler, H., Griesinger, C., Lautz, J., Muller, A., van Gunsteren, W. F., Berendsen, H. J. C. 1988. *J. Am. Chem. Soc.* 110:3393–96
71. Wüthrich, K., Billeter, M., Braun, W. 1983. *J. Mol. Biol.* 169:949–61
72. Clore, G. M., Gronenborn, A. M., Brünger, A. T., Karplus, M. 1985. *J. Mol. Biol.* 186:435–55
73. Holak, T. A., Prestegard, J. H., Forman, J. D. 1987. *Biochemistry* 4652–60
74. Pardi, A., Hare, D. R., Selsted, M. E., Morrison, R. D., Bassolino, D. A.,

Bach, A. C. II. 1988. *J. Mol. Biol.* 201:625–36
75. Nilges, M., Clore, G. M., Gronenborn, A. M. 1988. *FEBS Lett.* 239:129–36
76a. Zuiderweg, E. R. P., Boelens, R., Kaptein, R. 1985. *Biopolymers* 24:601–11
76b. LeMaster, D. M. 1987. *FEBS Lett.* 223:191–96
77. Driscoll, P. C., Clore, G. M., Beress, L., Gronenborn, A. M. 1989. *Biochemistry.* In press
78. Folkers, P. J. M., Clore, G. M., Driscoll, P. C., Dodt, J., Kohler, S., Gronenborn, A. M. 1989. *Biochemistry.* In press
79a. LeMaster, D. M., Kay, L. E., Brünger, A. T., Prestegard, J. H. 1988. *FEBS Lett.* 236:71–76
79b. Keepers, J. W., James, T. L. 1984. *J. Magn. Reson.* 57:404–26
80. Zhou, N. Z., Bianucci, A. M., Pattabiraman, N., James, T. L. 1987. *Biochemistry* 26:7905–13
81. Marion, D., Genest, M., Ptak, M. 1987. *Biophys. Chem.* 28:235–44
82. Brünger, A. T., Clore, G. M., Gronenborn, A. M., Karplus, M. 1986. *Proc. Natl. Acad. Sci. USA* 83:3801–5
83. Clore, G. M., Brünger, A. T., Karplus, M., Gronenborn, A. M. 1986. *J. Mol. Biol.* 191:523–51
84. Clore, G. M., Nilges, M., Brünger, A. T., Karplus, M., Gronenborn, A. M. 1987. *FEBS Lett.* 213:269–77
85. Nilges, M., Gronenborn, A. M., Brünger, A. T., Clore, G. M. 1988. *Protein Eng.* 2:27–38
86. Havel, T. F., Wüthrich, K. 1984. *Bull. Math. Biol.* 46:673–98
87. Havel, T. F., Wüthrich, K. 1985. *J. Mol. Biol.* 182:281–94
88. Braun, W., Go, N. 1985. *J. Mol. Biol.* 186:611–26
89. Wagner, G., Braun, W., Havel, T. F., Schaumann, T., Go, N., Wüthrich, K. 1987. *J. Mol. Biol.* 196:611–39
90. Kaptein, R., Zuiderweg, E. R. P., Scheek, R., Boelens, R., van Gunsteren, W. F. 1985. *J. Mol. Biol.* 182:179–82
91. Blumenthal, L. M. 1970. *Theory and Applications of Distance Geometry.* New York: Chelsea.
92. Kuntz, I. D., Crippen, G. M., Kollman, P. A., Kimelman, D. 1976. *J. Mol. Biol.* 106:983–94
93. Kuntz, I. D., Crippen, G. M., Kollman, P. A. 1979. *Biopolymers* 18:939–57
94. Crippen, G. M. 1977. *J. Comp. Phys.* 24:96–107
95. Crippen, G. M., Havel, T. F. 1978. *Acta Crystallogr. A* 34:282–84
96. Wako, H., Scheraga, H. A. 1982. *J. Protein Chem.* 1:85–117
97. Sippl, M. J., Scheraga, H. A. 1986. *Proc. Natl. Acad. Sci. USA* 83:2283–87
98. McCammon, J. A., Gelin, B. R., Karplus, M. 1977. *Nature* 267:585–90
99. McCammon, J. A., Wolyness, P. G., Karplus, M. 1979. *Biochemistry* 18: 927–42
100. Karplus, M., McCammon, J. A. 1983. *Annu. Rev. Biochem.* 52:263–300
101. Levitt, M. 1983. *J. Mol. Biol.* 170:723–64
102. Kaptein, R., Zuiderweg, E. R. P., Scheek, R. M., Boelens, R., van Gunsteren, W. F. 1985. *J. Mol. Biol.* 182:179–82
103. Clore, G. M., Gronenborn, A. M., Brünger, A. T., Karplus, M. 1985. *J. Mol. Biol.* 186:435–55
104. Clore, G. M., Nilges, M., Sukumaran, D. K., Brünger, A. T., Karplus, M., Gronenborn, A. M. 1986. *EMBO J.* 5:2729–35
105. Clore, G. M., Gronenborn, A. M., Nilges, M., Ryan, C. A. 1987. *Biochemistry* 26:8012–23
106. Zuiderweg, E. R. P., Scheek, R. M., Boelens, R., van Gunsteren, W. F., Kaptein, R. 1985. *Biochimie* 67:707–15
107. Kirkpatrick, S., Gelatt, C. D., Vecchi, M. P. 1983. *Science* 220:671–80
108. Nilges, M., Clore, G. M., Gronenborn, A. M. 1988. *FEBS Lett.* 229:317–24
109. Clore, G. M., Gronenborn, A. M., Kjaer, M., Poulsen, F. M. 1987. *Protein Eng.* 1:305–11
110. Clore, G. M., Gronenborn, A. M., James, M. N. G., Kjaer, M., McPhalen, C. A., Poulsen, F. M. 1987. *Protein Eng.* 1:313–18
111. Montelione, G. T., Wüthrich, K., Nice, E. C., Burgess, A. W., Scheraga, H. A. 1987. *Proc. Natl. Acad. Sci. USA* 84:5226–30
112. Kohda, D., Go, N., Hayashi, K., Inagaki, F. 1988. *J. Biochem.* 103:741–43
113. Kohda, D., Inagaki, F. 1988. *J. Biochem.* 103:554–71
114. Carver, J. A., Cooke, R. M., Esposito, G., Campbell, I. D., Gregory, H., Sheard, B. 1986. *FEBS Lett.* 205:77–81
115. Cooke, R. M., Wilkinson, A. J., Baron, M., Pastore, A., Tappin, M. J., et al. 1987. *Nature* 327:339–41
116. Frey, M. H., Wagner, G., Vasak, M., Sørensen, O. W., Neuhaus, D., et al. 1985. *J. Am. Chem. Soc.* 107:6847–51
117. Otvos, J. D., Engeseth, H. R., Wehrli, S. 1985. *J. Magn. Reson.* 61:579–84
118. Live, D., Armitage, I. M., Dalgarno, D. C., Cowburn, D. J. 1985. *J. Am. Chem. Soc.* 107:1775–77

119. Furey, W. F., Robbins, A. H., Clancy, L. L., Winge, D. R., Wang, B. C., Stout, C. D. 1986. *Science* 231:704–10
120. Furey, W. F., Robbins, A. H., Clancy, L. L., Winge, D. R., Wang, B. C., Stout, C. D. 1987. *Metallothionein II*, ed. J. H. R. Kägi, Y. Kojima, pp. 139–48. Basel:Birkhäuser
121. Nettesheim, D. G., Edalji, R. P., Mollison, K. W., Greer, J., Zuiderweg, E. R. P. 1988. *Proc. Natl. Acad. Sci. USA* 85:5036–40
122. Inagaki, F., Hider, R. C., Hodges, S. J., Drake, A. F. 1985. *J. Mol. Biol.* 183:575–90
123. Basus, V. J., Billeter, M., Love, R. A., Stroud, R. M., Kuntz, I. D. 1988. *Biochemistry* 27:2763–71
124. Kosen, P. A., Finer-Moore, J., McCarthy, M. P., Basus, V. J. 1988. *Biochemistry* 27:2775–81
125a. Strop, P., Wider, G., Wüthrich, K. 1983. *J. Mol. Biol.* 166:641–65
125b. Frank, G. 1983. *J. Mol. Biol.* 166: 665–68
126. Wemmer, D. E., Kumar, N. V., Metrione, R. M., Lazdunski, M., Drobny, G., Kallenbach, N. R. 1986. *Biochemistry* 25:6842–49
127. Pflugrath, J., Wiegand, E., Huber, R., Vertesy, L. 1986. *J. Mol. Biol.* 189:383–86
128. Deleted in proof
129. Kline, A. D., Braun, W., Wüthrich, K. 1986. *J. Mol. Biol.* 189:377–82
130. Kline, A. D., Braun, W., Wüthrich, K. 1988. *J. Mol. Biol.* 204:675–724
131a. Driscoll, P. C., Hill, A. O., Redfield, C. 1987. *Eur. J. Biochem.* 170:279–92
131b. Chazin, W. J., Rance, M., Wright, P. E. 1988. *J. Mol. Biol.* 202:603–22
131c. Chazin, W. J., Wright, P. E. 1988. *J. Mol. Biol.* 202:623–36
132. Dyson, H. J., Holmgren, A., Wright, P. E. 1989. *Biochemistry*. In press
133. Saudek, V., Williams, R. J. P., Ramponi, G. 1988. *J. Mol. Biol.* 199:233–37
134. Weiss, M. A., Jeitler-Nilsson, A., Fischbein, N. J., Karplus, M., Sauer, R. T. 1986. In *NMR in the Life Sciences*, ed. E. M. Bradbury, C. Nicolini, 107:37–48. *NATO ASI Ser.* London: Plenum
135. Griffey, R. H., Redfield, A. G., Loomis, R. E., Dahlquist, F. W. 1985. *Biochemistry* 24:817–22
136. LeMaster, D. M., Richards, F. M. 1985. *Biochemistry* 24:7263–68
137. Torchia, D. A., Sparks, S. W., Bax, A. 1988. *Biochemistry* 27:5135–41
138. Griffey, R. H., Redfield, A. G. 1987. *Q. Rev. Biophys.* 19:51–82
139. Kainoshi, M., Tsuji, T. 1982. *Biochemistry* 21:6273–79
140. Bendall, M. R., Pegg, D. T., Doddrell, D. M. 1983. *J. Magn. Reson.* 52:81–117
141. Bax, A., Griffey, R. H., Hawkins, B. L. 1983. *J. Magn. Reson.* 55:301–15
142. Griffey, R. H., Poulter, C. D., Bax, A., Hawkins, B. L., Yamaizumi, Z., Nishimura, S. 1983. *Proc. Natl. Acad. Sci. USA* 80:5895–97
143. Roy, S., Redfield, A. G., Papastavros, M. Z., Sanchez, V. 1984. *Biochemistry* 23:4395–400
144. Griffey, R. H., Redfield, A. G., McIntosh, L. P., Oas, T. G., Dahlquist, F. W. 1986. *J. Am. Chem. Soc.* 108:6816–17
145. Markley, J. L., Putter, I., Jardetzky, O. 1968. *Science* 161:1249–51
146. Kalbitzer, H. R., Leberman, R., Wittinghofer, A. 1985. *FEBS Lett.* 180:40–42
147. Torchia, D. A., Sparks, S. W., Bax, A. 1988. *J. Am. Chem. Soc.* 110:2320–21
148. Freeman, R., Mareci, T. H., Morris, G. A. 1981. *J. Magn. Reson.* 42:341–45
149. Bax, A., Weiss, M. A. 1987. *J. Magn. Reson.* 71:571–75
150. Senn, H., Otting, G., Wüthrich, K. 1987. *J. Am. Chem. Soc.* 109:1090–92
151. Rance, M., Wright, P. E., Messerle, B. A., Field, L. D. 1987. *J. Am. Chem. Soc.* 109:1591–93
152. Fesik, S. W., Gampe, R. T., Rockway, T. W. 1987. *J. Magn. Reson.* 74:366–71
153. McIntosh, L. P., Dahlquist, F. W., Redfield, A. G. 1987. *J. Biomol. Struct. Dyn.* 5:21–34
154. Gronenborn, A. M., Bax, A., Wingfield, P. T., Clore, G. M. 1989. *FEBS Lett.* In press
155. Markley, J. L. 1989. In *Methods in Enzymology*, ed. T. L. James, N. Oppenheimer. In press
156. Oh, B. H., Westler, W. M., Darba, P., Markley, J. L. 1988. *Science* 240:908–11
157. Westler, W. M., Stockman, B. J., Hosoya, Y., Miyake, Y., Kainosho, M., Markley, J. L. 1988. *J. Am. Chem. Soc.* 110:6256–58
158. Stockman, B. J., Reily, M. D., Westler, W. M., Ulrich, E. L., Markley, J. L. 1989. *Biochemistry* 28:230–36
159. Westler, W. M., Kainosho, M., Nagao, H., Tomonaga, N., Markley, J. L. 1988. *J. Am. Chem. Soc.* 110:4093–95

160. Bax, A., Sparks, S. W., Torchia, D. A. 1988. *J. Am. Chem. Soc.* 110:7926–27
161. Clore, G. M., Bax, A., Wingfield, P., Gronenborn, A. M. 1988. *FEBS Lett.* 238:17–21
162. Vuister, G. W., Boelens, R. 1987. *J. Magn. Reson.* 73:328–33
163. Griesinger, C., Sørensen, O. W., Ernst, R. R. 1988. *J. Magn. Reson.* 73:574–79
164. Griesinger, C., Sørensen, O. W., Ernst, R. R. 1987. *J. Am. Chem. Soc.* 109:7227–29
165. Oschkinat, H., Griesinger, C., Kraulis, P. J., Sørensen, O. W., Ernst, R. R., et al. 1988. *Nature* 332:374–76
166. Vuister, G. W., Boelens, R., Kaptein, R. 1988. *J. Magn. Reson.* 80:176–85
167. Fesik, S. W., Zuiderweg, E. R. P. 1988. *J. Magn. Reson.* 78:588–93
168. Braun, W., Wider, G., Lee, K. H., Wüthrich, K. 1983. *J. Mol. Biol.* 169:921–48
169. Brown, L. R., Braun, W., Kumar, A., Wüthrich, K. 1982. *Biophys. J.* 37:19–32
170. Schiksnis, R. A., Bogusky, M. J., Tsang, P., Opella, S. J. 1987. *Biochemistry* 26:1373–81
171. Boelens, R., Scheek, R. M., Lamerichs, R. M. J. N., de Vlieg, J., van Boom, J. H., Kaptein, R. 1987. *J. Mol. Biol.* 193:213–16
172. Marion, D., Kay, L. E., Sparks, S. W., Torchia, D. A., Bax, A. 1989. *J. Am. Chem. Soc.* In press
173. Bax, A., Sklenar, V., Gronenborn, A. M., Clore, G. M. 1987. *J. Am. Chem. Soc.* 109:6511–13